

# Initial perturbations dependence of non-equilibrium continuous and discontinuous pattern transition

Rikuya Ishikawa and Rei Kurita<sup>1</sup>

<sup>1</sup>*Department of Physics, Tokyo Metropolitan University,  
1-1 Minamioosawa, Hachioji-shi, Tokyo 192-0397, Japan*

(Dated: October 3, 2023)

A phase separation in a spatially heterogeneous environment is closely related to intracellular science and material science. For the phase separation, initial heterogeneous perturbations play an important role in pattern formations. In this study, a pattern transition from a lamellar pattern to a columnar pattern is investigated in the presence of a slit pattern as the initial perturbations. Here it is found that the transition behavior depends on the initial slit width. When the initial slit width is close to the width of the columnar pattern at the steady state, the pattern transition is the second-order-like (continuous) transition. Meanwhile, the pattern transition becomes the first-order-like (discontinuous) transition if the width of the initial slit is much larger than that at the steady state. Then those transition behaviors can be explained by the dynamical path during the pattern formation. This finding will advance understanding of the initial perturbation dependence of nonequilibrium phenomena.

## I. INTRODUCTION

A phase separation (PS) in which two phases are separated from a mixture is important in a wide range of fields such as material performance and biological activities [1–5]. For example, it is known that SnPb alloy used as solder exhibits phase separation and the formation of phase-separated domains may facilitate the formation of cracks at phase boundaries, resulting mechanical failure [6]. Moreover, it has been reported that protein droplets formed by the liquid-liquid phase separation (LLPS) in cells play important roles in transcription [7], signal transduction [8], and the pathogenesis of neurodegenerative diseases [9, 10].

Phase separation in binary mixtures has long been studied as a classical problem, and the dynamics of phase separation appears to be well understood both experimentally and theoretically [1, 4]. However, the universality of the dynamics holds for spatially uniform systems, but not for systems with inhomogeneous temperatures or concentrations. For example, in the case of an inhomogeneous system with large initial concentration fluctuations, a concentric pattern is formed around high concentration areas [11]. In the case of non-stationary temperature fields such as directional quenching (DQ) [12–15], a random droplet, lamellar and columnar pattern are formed depending on a migration speed  $V$  of a quenching front. There are many other examples for showing specific pattern formations in systems such as PS with radial quenching [16–18], PS with temperature gradient [19, 20], PS with lamination [21], PS with double quenching [22], PS with containing particles [23–26], particles creation [27], self-propelled systems [28], and non-reciprocal interaction systems [29]. Understanding of the phase separation phenomena under such inhomogeneous conditions is an urgent issue since the pattern formation are related with development of new functional materials and LLPS in cells occurs in inhomogeneous concentration

and temperature.

Although the importance of initial perturbations has been suggested for the pattern formation, there are few quantitative studies on the effects of the initial perturbations on a transition point and a transition behavior. Understanding the effects of the initial perturbations that cause transitions will not only facilitate the understanding of nonequilibrium systems, but also control the transitions which will be useful for applications in various fields. Therefore, we investigated the effect of the initial perturbations for the transition from columnar pattern to lamellar pattern in DQ. In this study, we prepared a slit pattern into the lamellar pattern as initial perturbations and studied a process of the transition from the columnar pattern to the lamellar pattern. It was found that the transition behavior depends on the slits width  $h$  and it means that the condition of the initial perturbation plays a critical role for the pattern formation.

## II. METHODS

In this study, we used modified-Cahn-Hilliard equation for understanding a dynamics of two dimensional phase separation under inhomogeneous temperature fields [1, 30]. The normalized equation of the modified-Cahn-Hilliard equation is given as

$$\frac{\partial \phi}{\partial t} = \nabla^2[\epsilon(x, t)\phi + \phi^3 - \nabla^2 \phi] \quad (1)$$

where  $\phi, t$  and  $\epsilon$  are the normalized concentration, the time normalized by the diffusion time and the temperature normalized by the quench depth, respectively. The length is normalized by the correlation length. We note that the effect of temperature gradient (Ludwig-Soret effect) was neglected. When  $\epsilon \geq 0$ , the mixed state is stable; when  $\epsilon < 0$ , the mixture is separated into two phases. In this study, we define  $\phi = 1$  and  $\phi = -1$  which

are the concentrations after phase separation as A (white region) and B phase (black region), respectively. To compute eq. 1, we used the Euler method and set a grid size to  $\Delta x = 1$  and a time increment to  $\Delta t = 0.01$ . We used a free surface condition in the  $x$  directions and a periodic boundary condition in the  $y$  directions. The system size is  $L_x : L_y = 1000 : 1000$ .

We initially put A phase in  $x < 40$  and then we put one or two slits of B phase in A phase as the initial perturbations (see Fig. 2). The width of one slit or the period of two slits is  $h$ . The region  $x \geq 40$  is a symmetric composition  $\phi = 0$ . Then, the quenching front was set to  $x = 40$  and annealed for  $-10 < t < 0$  to smooth the slit boundary of  $\phi$ . Even after the annealing, the width of the slit was confirmed to be  $h$ . At  $t = 0$ , the quenching front moved in the  $x$  direction with a constant velocity  $V$ . Therefore, the temperature  $\epsilon(x, t)$  is as follows.

$$\epsilon(x, t) = \begin{cases} 1 & x \geq Vt + 40 \\ -1 & x < Vt + 40 \end{cases}, \quad x \in [0, L_x - 1] \quad (2)$$

### III. RESULTS

Firstly, we describe the pattern formation when the quenching front is moved at  $V$  in the slit systems. We defined ‘‘columnar pattern’’ when columns percolate to the right boundary of the simulation box, while ‘‘lamellar pattern’’ is stable when the columns change into the lamellae during the pattern formation. We set the transition velocity  $V_t$  at the median of the lowest velocity for the lamellar pattern and the highest velocity for the columnar pattern. Figure 1 shows the  $h$  dependence of  $V_t$  in one or two slits system. There are two types of the transitions; one is a discontinuous transition (DT) and the other is a continuous transition (CT). We will describe the difference between DT and CT in the next paragraph. Circles, triangles, and diamonds correspond to  $V_t$  with DT for one slit, with CT for two slits, and with DT for two slits, respectively. For the one slit system, the  $V_t$  line is smooth with a peak at  $h = 9$  and the CT cannot be observed. Meanwhile, for the two slits system,  $V_t$  is larger for  $h \leq 9$  (triangle symbols) than for one slit system. For  $h \geq 10$  (diamond symbols),  $V_t$  with DT was almost the same as  $V_t$  with DT in the one slit system. In the following, we will reveal the reason for the large  $V_t$  jump around  $h = 9$  in the two slits case and we will discuss the difference from the one slit case.

Next, we describe  $h$  dependence of the pattern formation in the two slits case. Figure 2 shows the pattern formations for different  $h$ . For  $h = 8$  and  $V = 0.665$  just above  $V_t$ , the number of the slit increases as columns, but the columns break off in the middle and the lamellae are formed; the column formation have a finite lifetime (or a finite distance). Meanwhile, for  $h = 8$  and  $V = 0.66$  just below  $V_t$ , the columnar pattern percolates to the right boundary and the number of the column gradually increases. For the slits width  $h = 20$  and  $V =$

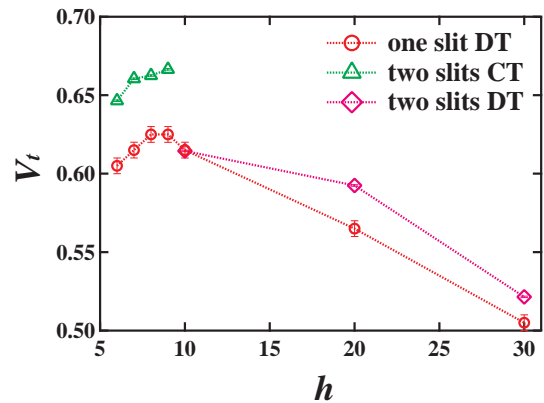


FIG. 1.  $h$  dependence of  $V_t$ . Circles, triangles, and diamonds correspond to  $V_t$  with a discontinuous transition (DT) for one slit, with a continuous transition (CT) for two slits, and with a DT for two slits, respectively. We set the transition velocity  $V_t$  at the median of the lowest velocity for the lamellar pattern and the highest velocity for the columnar pattern. An error bar represents the lowest velocity for the lamellar pattern and the highest velocity for the columnar pattern.

0.595 just above  $V_t$ , no column is generated from the slits and only lamellae are formed immediately after the DQ starts. Meanwhile, for  $h = 20$  and  $V = 0.59$  just below  $V_t$ , a thin column is formed at  $t = 200$  and then the number of the thin column increases and the columnar pattern percolates to the right boundary. Here we defined the continuous transition (CT) when the columns and lamellae coexist with some length like the system with  $h = 8$ , while the discontinuous transition (DT) when the lamellae are formed immediately.

In addition, to clarify the mode of the transition, we investigated the growing behavior of the column pattern just below  $V_t$ . When the quenching front migrates toward  $x$  direction, the lamellae are basically formed, but the column pattern also grows inside the lamellae (see Fig. 2). We defined a lamella and a column as one pair of A and B phase, and the number of lamellae and columns as  $n_l$ ,  $n_c$ , respectively. Figure 3 (a) and (b) show the  $n_c$  dependence of  $n_l$  for  $h = 8$  and 20, respectively. For  $h = 8$ ,  $n_c$  linearly increases at any  $V$ . When  $V$  is small, the slope  $a$  is about 2, which indicates that two columns are formed each time one lamella formed. As  $V$  approaches  $V_t$ , the slope decreases. Meanwhile, for  $h = 20$ , the slope changes when the initial thick slit changes to the thin column near  $V = V_t$ . It is also found that the slopes in the later period are almost constant. We investigate the  $a$  dependence on the velocity difference from  $V_t$   $\delta (= V_t - V)$  shown as in Fig. 3(c). Circles and squares correspond to  $a$  in  $h = 8$  and 20, respectively. Error bars reflect the errors in the linear fitting. For  $h = 8$ ,  $a$  obeys with  $\delta^\alpha$  and the power  $\alpha$  is about 0.40. The physical meaning of  $\alpha$  is unclear, thus the theoretical derivation of this relationship is a future work. For  $h = 20$ ,  $a$  has a non-zero value even  $\delta \rightarrow 0$ . Thus, the growth behaviors of the

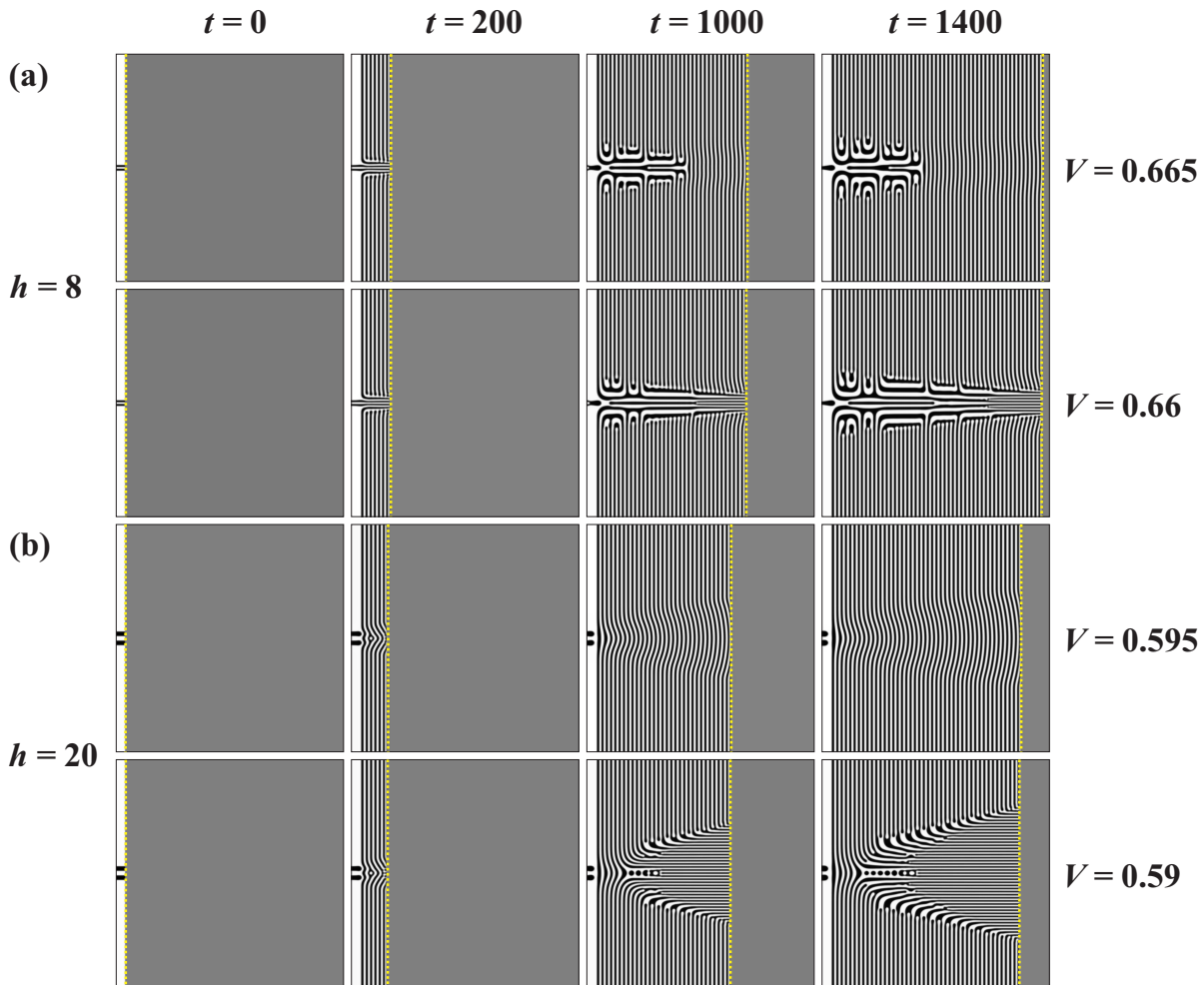


FIG. 2. Time evolution of patterns in two slits. The yellow dotted lines represent the quenching front. (a) For  $h = 8$  and  $V = 0.665$  just above  $V_t$ , the number of the slit increases as columns, but they break off in the middle and lamellae are formed; the column formation has a finite lifetime (or a finite distance). Meanwhile, for  $h = 8$  and  $V = 0.66$  just below  $V_t$ , the columnar pattern percolate to the right boundary and the number of the column gradually increases. (b) For the slits width  $h = 20$  and  $V = 0.595$  just above  $V_t$ , no column is generated from the slits and only lamellae are formed immediately. Meanwhile, for  $h = 20$  and  $V = 0.59$  just below  $V_t$ , a thin column is formed at  $t = 200$  and then the number of the thin column increases and the columnar pattern percolates to the right boundary.

column pattern depend on  $\delta$  and there is a clear difference between CT ( $h = 8$ ) and DT ( $h = 20$ ).

We also show the pattern formation behaviors above  $V_t$ . To clarify the dynamics in CT, we investigated the coexistence length of the columns and the lamellae for  $h = 8$ . We define  $\xi$  as the distance from the initial position of the slit to the vanishing point of the columns (see Fig. 4 (a)) and investigate  $\xi$  dependence on  $|\delta| (= V - V_t)$  shown as in Figure 4(b).  $\xi$  diverges as  $\xi \sim |\delta|^\beta$  with decreasing  $|\delta|$  and  $\beta$  is about -0.50. This behavior also suggests that the pattern transition at  $V = V_t$  should be continuous at  $h = 8$ . Meanwhile,  $\xi = 0$  at  $h = 20$  as we noted above (see Fig. 2(b)).

Here we investigated the time evolution of the concentration at a position prior to the quenching front of the column in order to reveal the formation dynamics in the

continuous transition. Figure 5(a) shows the time evolution of  $\phi(x_f + 3, y)$  at  $h = 8$  and  $V = 0.663$ , where  $x_f$  is a position of the quenching front at  $t$ . We also define the  $y$ -coordinate of the center of the column as  $y_c$  (indicated by yellow dotted line) and  $\phi(x_f + 3, y_c)$  is denoted by  $\phi_{fc}$  in the following. Since the concentration is conserved and A phase rich ahead of the column with B phase,  $\phi_{fc}$  is positive (A rich phase), while the column is composed by B phase. As time passed,  $\phi_{fc}$  periodically changes shown as in Fig. 5(b). Circles, squares and triangles are  $V = 0.66, 0.663, \text{ and } 0.665$ , respectively. When  $V$  is smaller than  $V_t = 0.6625$  ( $V = 0.66$ ), the amplitude of  $\phi_{fc}$  oscillation is quite small at any  $t$ . Meanwhile, when  $V$  is larger than  $V_t$  ( $V = 0.663$  and  $0.665$ ), the oscillations of  $\phi_{fc}$  become larger with time and then the column finally transforms into lamellae.

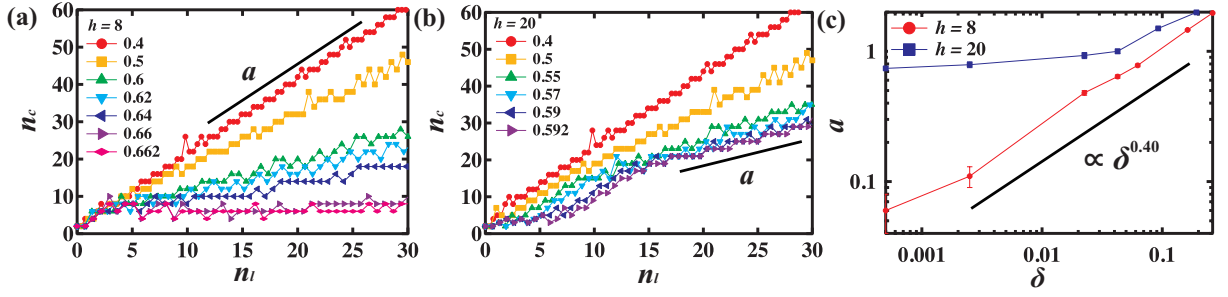


FIG. 3.  $n_c$  dependence on  $n_l$  for (a)  $h = 8$  and for (b)  $h = 20$ . Each symbols represent  $n_c$  in a different  $V$ . For  $h = 8$ ,  $n_c$  linearly increases at any  $V$  and the slope decreases with increasing  $V$ . For  $h = 20$ , the slope change at the time of the changing from thick slits to thin column when  $V$  is close to  $V_t$  and the slope in the later period are almost constant near  $V_t$ . (c)  $\delta (= V_t - V)$  dependence of the slope  $a$  in log-log scales. Circles and squares correspond to  $h = 8$  and  $20$ , respectively. For  $h = 8$ ,  $a$  obeys with  $\delta^\alpha$  and the power  $\alpha$  is about 0.40. For  $h = 20$ ,  $a$  has a finite value even  $\delta \rightarrow 0$ . The  $a$  dependence of  $\delta$  also suggests the difference between CT and DT modes.

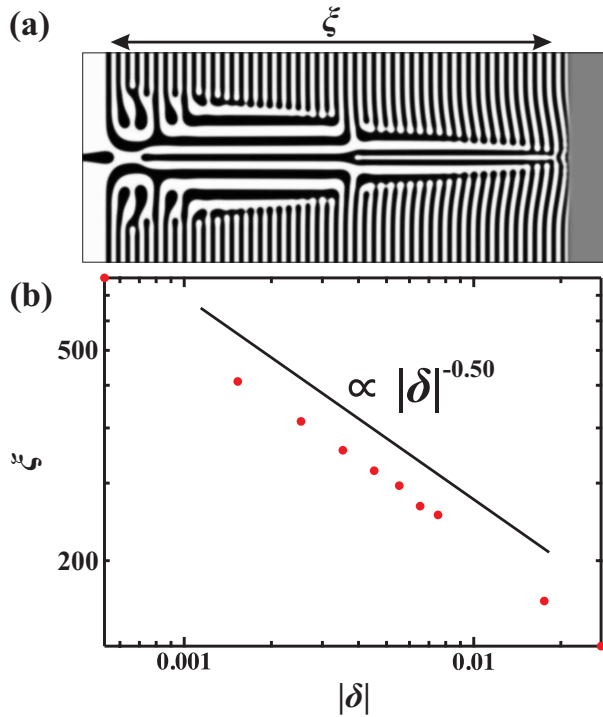


FIG. 4. (a) We define  $\xi$  as the distance from the initial position of the slit to the vanishing point of the columns at  $h = 8$ . (b)  $|\delta|$  dependence of  $\xi$ .  $\xi$  diverges as  $\xi \sim |\delta|^\beta$  with decreasing  $|\delta|$  and  $\beta$  is about -0.50. This behavior also suggests that the pattern transition at  $V = V_t$  should be continuous at  $h = 8$ .

Here, we considered the periodic fluctuations and divergence of  $\phi_{fc}$ . Due to the conserved manner, A component accumulates in front of the B phase columns ( $\phi_{fc} > 0$  in front of the B column). When B phase columns grow, the accumulated A component is diffused in the lateral direction. When a lamella of A phase is formed next to B phase column, a layer with  $\phi < 0$  is formed in front of the quenching front. Then the accumulated A component in front of the B phase columns

tends to diffuse the laterally since the difference of  $\phi$  is large. Thus,  $\phi_{fc}$  oscillates slightly with the same period as the period of the lamella. Next, the quenching front movement is faster than the characteristic time of the diffusion when  $V \geq V_t$ . The A component is gradually accumulated in front of the B phase columns with time. The amplitude of the oscillation gradually increases and the onset time, when the amplitude of  $\phi_{fc}$  oscillation becomes larger, becomes shorter with increasing  $V$ . They are consistent that the accumulation of A component is faster than the diffusion. Therefore, the dynamics in CT is determined by the competition between the accumulation and the diffusion in front of the column.

When the width of the initial slit  $h$  is large, the thinner column is reformed during DQ. It means that the stable width of the column is mismatched with the width of the initial slit. Thus, we compute the stable width of the column here. According to the previous report in Ref. [21], a stable thickness of the lamella  $\xi'$  can be expressed as  $\xi' \sim V^{-1/2}$  since the time scales of the diffusion and the migration of the free surface are balanced. Similarly, the stable width of the column is expected to be determined by the competition between the velocity of the quenching front and the speed of the diffusion. We investigated the  $V$  dependence of the stable width of the column  $\lambda$  just after the entire system was quenched. Figure 6 shows the  $V$  dependence of  $\lambda$ . Circles and triangles are  $h = 8$  and  $20$ , respectively. Symbols and error bars are the mean and the standard deviation of  $\lambda$  for all columns, respectively. It is found that  $\lambda$  is independent of  $h$  and  $\lambda \propto V^{-0.60}$ . In the lamella pattern, the diffusion perpendicular to the quenching front is only considered, while the diffusion in both perpendicular and lateral direction should be related in the column pattern. Thus we consider that the exponent in the column pattern is different from that in the lamella pattern. When  $h$  is large and  $V < V_t$ , the wide initial slit branches into columns of the steady width  $\lambda$ . Meanwhile, when  $V \geq V_t$ , the diffusion is slower than the migration of quenching front. A layer of A component is formed in front of the B phase column

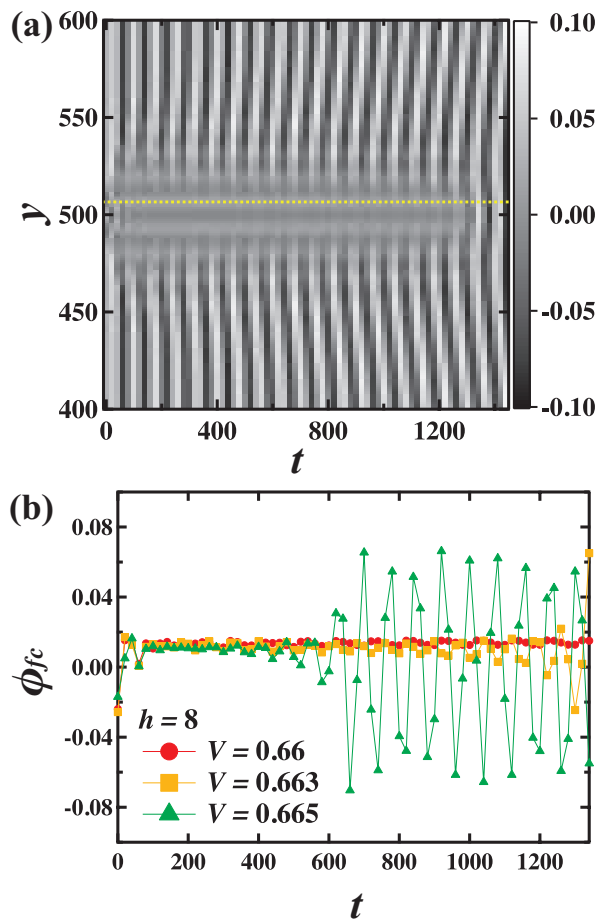


FIG. 5. (a) The time evolution of  $\phi(x_f + 3, y)$  at  $h = 8$  and  $V = 0.663$ , where  $x_f$  is a position of the quenching front at  $t$ .  $x_f$  and  $y_c$  show the  $x$ -coordinate of the quenching front and the  $y$ -coordinate of the column center (indicated by yellow dotted line), respectively. (b) Time evolution of  $\phi_{fc}$  at  $h = 8$ . Circles, squares and triangles are  $V = 0.666$ ,  $0.663$ , and  $0.665$ , respectively.  $V_t = 0.6625$  at  $h = 8$ . When  $V$  is smaller than  $V_t = 0.6625$  ( $V = 0.66$ ), the amplitude of  $\phi_{fc}$  oscillation is quite small at any  $t$ . Meanwhile, when  $V$  is larger than  $V_t$  ( $V = 0.663$  and  $0.665$ ), the oscillations of  $\phi_{fc}$  become larger with time and then the column finally transforms into lamellae. The dynamics in CT is determined by the competition between the accumulation and the diffusion in front of the column.

and then the layer becomes the stable lamellar pattern.

Finally, we explain the conditions under which CT occurs. Figure 7 is a superimposed graph of Fig. 1 and Fig. 6 with  $V$  on the vertical axis and  $h$  on the horizontal axis. Filled circles and filled squares are the stable column width  $\lambda$  at the initial slit width  $h = 8$  and  $20$ , respectively. There is a critical-like point  $(h, V) = (h_c, V_c)$ , where  $\lambda(V_c) = h_c$  and  $V_t(h_c) = V_c$ . Figure 7 is a state diagram and the transition modes between CT and DT can be explained by this diagram. As an example, we consider the case  $h = 15$  and  $V = 0.5$  (black circle). In this case, a misfit parameter between the initial slit and

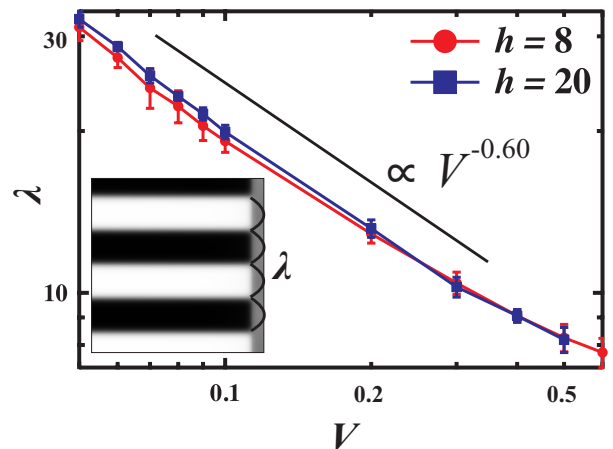


FIG. 6.  $V$  dependence of  $\lambda$  just after the entire system is quenched. Circles and triangles are  $h = 8$  and  $20$ , respectively. Symbols and error bars are the mean and standard deviation of  $\lambda$  for all columns, respectively. It is found that  $\lambda$  is independent of  $h$  and  $\lambda \propto V^{-0.60}$ .

the stable column  $\Delta h = h - \lambda$  is large. When  $V < V_t$ , the slits for  $h = 15$  branch to a column with  $\lambda = 8$  to eliminate this misfit. In the post-bifurcation state,  $\delta = V_t - V$  is also large and the ratio of column formation to lamella  $a$  is also large. Meanwhile, the slits immediately become a lamella if  $V > V_t$ . Therefore, due to the bifurcation, the condition cannot be close to the critical-like point and then the transition is discontinuous. Meanwhile,  $\lambda \sim h_c$  holds at  $h = 8$  and  $V = V_c$ . In this case, the condition of DQ is close to the critical-like point and the transition becomes continuous. We note here that if  $h$  is slightly larger than  $\lambda$ , the slits cannot branch. Therefore, we consider that the transition is the continuous up to  $h = 9$ .

In addition, we describe the difference of the transition mode between one slit and two slits. One slit is more likely to be lamellae than two slits because the upper and lower lamellae are closer together. Therefore,  $V_t$  for one slit is smaller than for two slits. If  $V < V_t$ , two or more columns are formed from one slit. When two or more columns are formed, the stability increases and then  $V_t$  becomes larger. Then, the condition becomes far from the critical-like point. We note that the state diagram for three or more slits is similar to that of two slits. Therefore, the stability of the pattern is unchanged after two or more columns are formed.

These results suggest that the stability of the system changes with the time dependent condition such as the number of the slit, the width of the slit or the column. Then the discontinuous transition occurs since the re-established transition point is farther away from the simulated state. Conversely, if the initial inhomogeneous perturbations are close to the stable state, the stability of the system is unchanged and then the continuous transition occurs near the critical point. It can be concluded that the difference between the initial inhomoge-

neous perturbations (the slit width  $h$  in this study) and the steady state (the column width  $\lambda$  in this study) significantly affects the mode of the pattern formation.

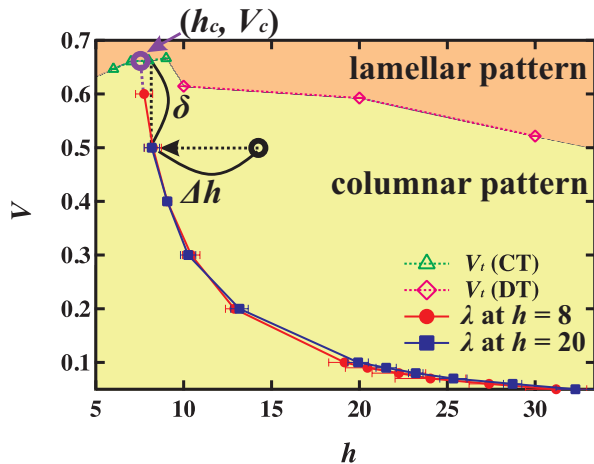


FIG. 7. A superimposed graph of Fig. 1 and Fig. 6 with  $V$  and  $h$ . The vertical and horizontal axis of Fig. 6 are swapped. Filled circles and filled squares are the column width  $\lambda$  at  $h = 8$  and  $20$ , respectively. There exists a critical-like point  $(h, V) = (h_c, V_c)$ , where  $\lambda$  and  $V_t$  curves cross. When the condition is close to the critical-like point, the transition is continuous. In the case  $h = 15$  and  $V = 0.5$  (black circle), a misfit parameter between the initial slit and the stable column  $\Delta h = h - \lambda$  is large. When  $V < V_t$ , the slits for  $h = 15$  branch to a column with  $\lambda = 8$  to eliminate this misfit. In the post-bifurcation state,  $\delta = V_t - V$  is also large and then the transition is discontinuous.

#### IV. DISCUSSION

Firstly, we discuss the relevance of this study with experimental studies on directional pattern formation during eutectic growth and gelation process. In metallic alloys, eutectic patterns have been observed to self-assemble perpendicular to the crystal-growth direction (like columnar pattern) when it solidifies in a certain direction [31–33]. However, a horizontal pattern (like lamellar pattern) is not formed with respect to the crystal-growth direction. Similarly, in gelation of collagen induced by directional neutralization, a pattern perpendicular to the gelation plane (like columnar pattern) is formed [34], but a horizontal pattern (like lamellar pattern) is not formed. In this study,  $V_t$  with the initial perturbations is about one order of magnitude larger than  $V_t$  in homogeneous DQ [14] and then the  $V$  regime of the lamellar pattern becomes narrow. Therefore, in nonequilibrium systems, the uncontrollable initial perturbations exist and then it seems difficult to observe lamellar patterns in experiments.

Next, we discuss the relationship between CT in DQ and the general critical phenomena. The results of the continuous transition in DQ are deterministic, not taking

into account thermal fluctuations. On the other hand, the critical phenomena of the phase transition [4] and a laminar-turbulent transition [35] are stochastic with thermal fluctuations. In fact, the columns do not disappear at the center of the columnar pattern, which is different from a critical phenomenon. Therefore, in this stage, the CT in DQ is different from these critical phenomena, and it is more appropriate to consider the pattern transition as interfacial dynamics.

Finally, the transition of the pattern formation under inhomogeneous conditions are not limited to phase separations, but also occur in other nonequilibrium systems such as active matter [36–38], non-reciprocal phase transitions [39], reversible-irreversible transitions in jamming systems [40, 41]. It is interesting that nonequilibrium continuous transition are observed in many systems such as the laminar-turbulent transition in fluids [35], two turbulent states in liquid crystals [42, 43] and a reversible-irreversible transition of fiber [44], vortices [45, 46] and granular materials [47]. Thus it is expected that the difference between the condition at the steady state and the initial perturbations plays an important role in those nonequilibrium transition.

#### V. SUMMARY

A phase separation is important in a wide range of fields such as material science and biology. Those phase separations often exhibit in inhomogeneous concentrations or non-stationary temperature fields. Understanding of phase separation phenomena under such inhomogeneous conditions is an urgent issue since LLPS in cells occurs in inhomogeneous concentration and temperature and the pattern formation are related with development of new functional materials.

Here, we investigated the columnar-lamellar pattern transition due to directional quenching (DQ) in the presence of initial slits pattern to study the effect of initial perturbations. In this study, we prepared one slit and two slits which are the nuclei of the columnar pattern as initial perturbations. Then, we studied the process of transition from columnar pattern to lamellar pattern dependent on the initial perturbations.

It is found that the transition behavior depends on the slit width  $h$  and the number of the slits. The transition from the column to the lamella is continuous when  $h$  is comparable to the column width  $\lambda$  and two slits. Then, the growth of the columnar pattern is determined by the balance between the diffusion and the accumulation of the concentration. Whereas, it is a discontinuous transition when  $h$  is larger than the column width  $\lambda$ . The stability of the system changes with the time dependent condition such as the number of the slit, the width of the slit or the column. Then the discontinuous transition occurs since the re-established transition point is farther away from the simulated state.

This study not only shows the empirically knowl-

edge that inhomogeneous initial perturbations can significantly change the transition point from a homogeneous system. It also shows that in nonequilibrium systems, the transition behaviors are determined by the difference between the initial perturbations and the condition at the steady state. Therefore, it is important to design initial perturbations comparing with the condition at the steady state in order to control pattern formation and nonequilibrium transitions in experiments.

#### ACKNOWLEDGEMENTS

R. I. was supported by JST SPRING, Grant Number JPMJSP2156. R. K. was supported by JSPS KAKENHI Grant Number 20H01874.

#### AUTHORS CONTRIBUTIONS

R. I. and R. K. conceived the project. R. I. performed the numerical simulations and analyzed the data. R. I.

and R. K. wrote the manuscript.

#### COMPETING INTERESTS STATEMENT

The authors declare that they have no competing interests.

#### CORRESPONDENCE

Correspondence and requests for materials should be addressed to R. I. (ishikawa-rikuya@tmu.ac.jp) and R. K. (kurita@tmu.ac.jp).

#### AVAILABILITY OF DATA AND MATERIALS

All data generated or analyzed during this study are included in this published article and its supplementary information files.

- 
- [1] J. W. Cahn and J. E. Hilliard, “Free energy of a nonuniform system. i. interfacial free energy,” *J. Chem. Phys.* **28**, 258–267 (1958).
- [2] Anthony A. Hyman, Christoph A. Weber, and Frank Jülicher, “Liquid-liquid phase separation in biology,” *Annu. Rev. Cell Dev. Biol.* **30**, 39–58 (2014).
- [3] M. C. Cross and P. C. Hohenberg, “Pattern formation outside of equilibrium,” *Rev. Mod. Phys.* **65**, 851–1112 (1993).
- [4] A. Onuki, *Phase Transition Dynamics* (Cambridge University Press, Cambridge, U.K., 2002).
- [5] I. W. Hamley, *Introduction to Soft Matter: Synthetic and Biological Self-Assembling Materials* (Wiley, Hoboken, NJ, 2007).
- [6] W. Dreyer and W. H. Müller, “Modeling diffusional coarsening in eutectic tin/lead solders: a quantitative approach,” *Int. J. Solids Struct.* **38**, 1433–1458 (2001).
- [7] Denes Hnisz, Krishna Shrinivas, Richard A. Young, Arup K. Chakraborty, and Phillip A. Sharp, “A phase separation model for transcriptional control,” *Cell* **169**, 13–23 (2017).
- [8] Xiaolei Su, Jonathon A. Ditlev, Enfu Hui, Wenmin Xing, Sudeep Banjade, Julia Okrut, David S. King, Jack Taunton, Michael K. Rosen, and Ronald D. Vale, “Phase separation of signaling molecules promotes t cell receptor signal transduction,” *Science* **352**, 595–599 (2016).
- [9] Susanne Wegmann, Bahareh Eftekharzadeh, Katharina Tepper, Katarzyna M Zoltowska, Rachel E Bennett, Simon Dujardin, Pawel R Laskowski, Danny MacKenzie, Tarun Kamath, Caitlin Commins, Charles Vanderburg, Allyson D Roe, Zhanyun Fan, Amandine M Molliex, Amayra Hernandez-Vega, Daniel Muller, Anthony A Hyman, Eckhard Mandelkow, J Paul Taylor, and Bradley T Hyman, “Tau protein liquid-liquid phase separation can initiate tau aggregation,” *EMBO J.* **37**, e98049 (2018).
- [10] Simon Alberti and Dorothee Dormann, “Liquid-liquid phase separation in disease,” *Annu. Rev. Genet.* **53**, 171–194 (2019).
- [11] Hiroshi Furukawa, “Concentric patterns in mesoscopic spinodal decomposition,” *J. Phys. Soc. Jpn.* **63**, 3744–3750 (1994).
- [12] Hiroshi Furukawa, “Phase separation by directional quenching and morphological transition,” *Physica A* **180**, 128–155 (1992).
- [13] Alexei Krekhov, “Formation of regular structures in the process of phase separation,” *Phys. Rev. E* **79**, 035302(R) (2009).
- [14] Tsuyoshi Tsukada and Rei Kurita, “Mechanism behind columnar pattern formation during directional quenching-induced phase separation,” *Phys. Rev. Res.* **2**, 013382– (2020).
- [15] Rikuya Ishikawa, Marie Tani, and Rei Kurita, “Three-dimensional phase separation under a nonstationary temperature field,” *Phys. Rev. Res.* **4**, 033152– (2022).
- [16] R. Kurita, “Control of pattern formation during phase separation initiated by a propagated trigger,” *Sci. Rep.* **7**, 6912 (2017).
- [17] Tsuyoshi Tsukada and Rei Kurita, “Pattern formation during phase separation by radial quenching at the base of a three-dimensional box,” *J. Phys. Soc. Jpn.* **88**, 044603 (2019).
- [18] Tsuyoshi Tsukada and Rei Kurita, “Topological transition by confinement of a phase separating system with radial quenching,” *Sci. Rep.* **9**, 15764 (2019).
- [19] Sutapa Roy, Siegfried Dietrich, and Anna Maciolek, “Solvent coarsening around colloids driven by temperature gradients,” *Phys. Rev. E* **97**, 042603 (2018).
- [20] Sutapa Roy and Anna Maciolek, “Phase separation around heated colloid in bulk and under confinement,” *Soft Matter* **14**, 9326–9335 (2018).

- [21] Rikuya Ishikawa, Marie Tani, and Rei Kurita, “Selective 3-dimensional patterning during phase separation of a continuously laminated layer,” *Physica A* **622**, 128834 (2023).
- [22] Hajime Tanaka and Takeaki Araki, “Spontaneous double phase separation induced by rapid hydrodynamic coarsening in two-dimensional fluid mixtures,” *Phys. Rev. Lett.* **81**, 389–392 (1998).
- [23] Hajime Tanaka, Andrew J. Lovinger, and Don D. Davis, “Pattern evolution caused by dynamic coupling between wetting and phase separation in binary liquid mixture containing glass particles,” *Phys. Rev. Lett.* **72**, 2581–2584 (1994).
- [24] Takeaki Araki and Shintaro Fukai, “Controlled motion of janus particles in periodically phase-separating binary fluids,” *Soft Matter* **11**, 3470–3479 (2015).
- [25] Takeaki Araki and Hajime Tanaka, “Wetting-induced depletion interaction between particles in a phase-separating liquid mixture,” *Phys. Rev. E* **73**, 061506– (2006).
- [26] Alexei Krekhov, Vanessa Weith, and Walter Zimmermann, “Periodic structures in binary mixtures enforced by janus particles,” *Phys. Rev. E* **88**, 040302(R) (2013).
- [27] Kyosuke Adachi and Kyogo Kawaguchi, “Surface wetting by kinetic control of liquid-liquid phase separation,” *Phys. Rev. E* **104**, L042801– (2021).
- [28] Michael E. Cates and Julien Tailleur, “Motility-induced phase separation,” *Annu. Rev. Condens. Matter Phys.* **6**, 219–244 (2015).
- [29] Suropriya Saha, Jaime Agudo-Canalejo, and Ramin Golestanian, “Scalar active mixtures: The nonreciprocal cahn-hilliard model,” *Phys. Rev. X* **10**, 041009– (2020).
- [30] Prabhat K. Jaiswal, Sanjay Puri, and Kurt Binder, “Phase separation in thin films: Effect of temperature gradients,” *Europhys. Lett.* **103**, 66003 (2013).
- [31] Marie Ginibre, Silvère Akamatsu, and Gabriel Faivre, “Experimental determination of the stability diagram of a lamellar eutectic growth front,” *Phys. Rev. E* **56**, 780–796 (1997).
- [32] Kenneth Jackson and J Hunt, “Lamellar and rod eutectic growth,” *Trans. Met. Soc. AIME* **236**, 1129–1141 (1966).
- [33] Ashish A. Kulkarni, Julia Kohanek, Kaitlin I. Tyler, Erik Hanson, Dong-Uk Kim, Katsuyo Thornton, and Paul V. Braun, “Template-directed solidification of eutectic optical materials,” *Adv. Opt. Mater.* **6**, 1800071 (2018).
- [34] Junta Yonemoto, Yasuyuki Maki, Isabel Koh, Kazuya Furusawa, and Masahiko Annaka, “Formation of multi-channel collagen gels investigated using particle tracking microrheology,” *Biomacromolecules* **22**, 3819–3826 (2021).
- [35] Masaki Sano and Keiichi Tamai, “A universal transition to turbulence in channel flow,” *Nat. Phys.* **12**, 249–253 (2016).
- [36] Tamás Vicsek, András Czirók, Eshel Ben-Jacob, Inon Cohen, and Ofer Shochet, “Novel type of phase transition in a system of self-driven particles,” *Phys. Rev. Lett.* **75**, 1226–1229 (1995).
- [37] Francesco Ginelli, “The physics of the vicsek model,” *Eur. Phys. J.: Spec. Top.* **225**, 2099–2117 (2016).
- [38] Hugues Chaté, “Dry aligning dilute active matter,” *Annu. Rev. Condens. Matter Phys.* **11**, 189–212 (2020).
- [39] Michel Fruchart, Ryo Hanai, Peter B. Littlewood, and Vincenzo Vitelli, “Non-reciprocal phase transitions,” *Nature (London)* **592**, 363–369 (2021).
- [40] Kentaro Nagasawa, Kunimasa Miyazaki, and Takeshi Kawasaki, “Classification of the reversible–irreversible transitions in particle trajectories across the jamming transition point,” *Soft Matter* **15**, 7557–7566 (2019).
- [41] C. Reichhardt, Ido Regev, K. Dahmen, S. Okuma, and C. J. O. Reichhardt, “Reversible to irreversible transitions in periodic driven many-body systems and future directions for classical and quantum systems,” *Phys. Rev. Res.* **5**, 021001– (2023).
- [42] Kazumasa A. Takeuchi, Masafumi Kuroda, Hugues Chaté, and Masaki Sano, “Directed percolation criticality in turbulent liquid crystals,” *Phys. Rev. Lett.* **99**, 234503– (2007).
- [43] Kazumasa A. Takeuchi, Masafumi Kuroda, Hugues Chaté, and Masaki Sano, “Experimental realization of directed percolation criticality in turbulent liquid crystals,” *Phys. Rev. E* **80**, 051116– (2009).
- [44] Alexandre Franceschini, Emmanouela Filippidi, Elisabeth Guazzelli, and David J. Pine, “Transverse alignment of fibers in a periodically sheared suspension: An absorbing phase transition with a slowly varying control parameter,” *Phys. Rev. Lett.* **107**, 250603– (2011).
- [45] S. Maegochi, K. Ienaga, and S. Okuma, “Critical behavior of density-driven and shear-driven reversible–irreversible transitions in cyclically sheared vortices,” *Sci. Rep.* **11**, 19280 (2021).
- [46] N. Mangan, C. Reichhardt, and C. J. Olson Reichhardt, “Reversible to irreversible flow transition in periodically driven vortices,” *Phys. Rev. Lett.* **100**, 187002– (2008).
- [47] Christopher Ness and Michael E. Cates, “Absorbing-state transitions in granular materials close to jamming,” *Phys. Rev. Lett.* **124**, 088004– (2020).